nature communications

Article

https://doi.org/10.1038/s41467-024-51962-x

Fine-tuning of IPA1 transactivation activity by E3 ligase IPI7-mediated non-proteolytic K29-ubiquitination during *Magnaporthe oryzae* infection

Received: 8 January 2024

Accepted: 20 August 2024

Published online: 01 September 2024

Check for updates

Hui Shi[1,6], Junjie Yin[1,6], Zhangjie Zhao[1,6], Hong Yu[2,6], Hong Yi[1], Li Xu[1], Huimin Tong[1], Min He[1], Xiaobo Zhu[1], Xiang Lu[1], Qing Xiong[1], Weitao Li[1,3], Yongyan Tang[1], Qingqing Hou[1], Li Song[1], Long Wang[1], Xiaoqiong Chen[1,3], Changhui Sun[1,3], Ting Li[1], Jing Fan[1], Yan Li[1], Peng Qin[1,3], Wen-Ming Wang[1], Shigui Li[1,3], Xuewei Chen[1], Jiayang Li[2,4] & Jing Wang[1,5]

The Ideal Plant Architecture 1 (IPA1) transcription factor promotes rice yield and immunity through phosphorylation at its amino acid residue Ser163 as a switch. Although phosphorylated IPA1 mimic, IPA1(S163D), directly targets the promoter of immune response gene *WRKY45*, it cannot activate its expression. Here, we identified a co-activator of IPA1(S163D), a RING-finger E3 ligase IPA1 interactor 7 (IPI7), which fine-tunes the transcriptional activity of IPA1 to timely promote plant immunity and simultaneously maintain growth for yield. IPI7 interacts with IPA1 and promotes K29-polyubiquitination of IPA1 in vitro and in vivo. However, the stability of IPA1 protein is not affected by IPI7-mediated ubiquitination. The IPI7-promoted K29-polyubiquitination of IPA1 is induced by *Magnaporthe oryzae* infection and required for phosphorylated IPA1 to transactivate *WRKY45* expression for immune response but not for plain IPA1 to transactivate *DENSE AND ERECT PANICLES 1* (*DEP1*) expression for panicle development. *IPI7* knockout impairs IPA1-mediated immunity but not yield. Our study reveals that plants utilize non-proteolytic K29-ubiquitination as a response to pathogen infection to fine-tune IPA1 transactivation activity for promoting immunity.

To protect themselves from pathogen attacks, plants have developed a sophisticated immune system that includes pathogen-associated molecular pattern (PAMP)-triggered immunity (PTI) and effector-triggered immunity (ETI)[1,2]. Plants can recognize different kinds of pathogens and rapidly activate immune signaling pathways within individual cells to trigger a series of events, such as activation of mitogen activated protein kinase (MAPK) cascades, induction of pathogenesis-related (*PR*) genes, production of reactive oxygen species (ROS), and deposition of callose and lignin[3].

[1]State Key Laboratory of Crop Gene Exploration and Utilization in Southwest China, Sichuan Agricultural University at Wenjiang, Chengdu 611130 Sichuan, China. [2]Key Laboratory of Seed Innovation, Institute of Genetics and Developmental Biology, Chinese Academy of Sciences, 100101 Beijing, China. [3]Rice Research Institute, Sichuan Agricultural University, Chengdu 611130, China. [4]Yazhouwan National Laboratory, Sanya 572024 Hainan, China. [5]College of Agronomy, Sichuan Agricultural University at Wenjiang, Chengdu 611130 Sichuan, China. [6]These authors contributed equally: Hui Shi, Junjie Yin, Zhangjie Zhao, Hong Yu. e-mail: jingwang406@sicau.edu.cn

Post-translational modifications (PTMs) are ubiquitous regulatory mechanisms critical for cell signaling transduction, regulating the molecular switches and crosstalk between linked pathways spatially and temporally. Ubiquitination is one of the major PTMs that regulates a wide range of cellular processes, including hormone signaling, cell cycle, plant senescence, flowering, plant architecture generation and the immune response[4–10]. Ubiquitination of a protein substrate requires a sequential activation of three enzymes: ubiquitin (Ub)-activating enzyme (E1), Ub-conjugating enzyme (E2), and Ub ligase (E3). Activated Ub is transferred from E1 to E2. Then, E2 forms a complex with E3 which transfers Ub to the substrate. The E1-E2-E3 enzymatic cascade is a repetitive process, resulting in the formation of mono-ubiquitin or a poly-Ub chain[11]. Ubiquitinated proteins undergo quite different fates depending on the number and site of the attached Ub molecules[12]. In plants, mono Ub in a cell can serve as a signal for endosomal punctual and histone structural change as well as protein stability[13–15]. The K48-linked poly-Ub chain is the first identified poly-Ub chain, helping the substrate to enter 26S proteasome for degradation[16]. Many non-K48-linked types of ubiquitination serve in non-proteolytic roles, such as K63-linked ubiquitination, that often function in regulation of protein stability, internalization and sorting[5,8,17]. Although a plethora of novel data have emerged regarding the molecular functions of mono-, K48-, and K63-ubiquitin chain, rarely studies reported on other ubiquitin chains, especially in the plant kingdom.

During the ubiquitination process, E3 ligases play a critical role in determining substrate specificity for target proteins. Based on their conserved domains, E3 ligases can be divided into various types, such as Really Interesting New Gene (RING)/U-box, Homology to E6-AP C Terminus (HECT), Anaphase Promoting Complex (APC), SKP1-CUL1-F-box (SCF), CUL3-BTB, and CUL4-DDB1-DWD[18]. These different types of E3 ligases have been identified to be involved in plant immune responses, including effector recognition, receptor complexes initiation, and immune signal transduction[19]. Many effectors, such as AvrPtoB, XopK and XopAE, require E3 ligase activity for full virulence of pathogens and for interaction with hosts[20–25]. Direct ubiquitination of pattern recognition receptors by E3 ligases can attenuate plant innate immunity. For example, flg22 induces two E3 ligases, PUB12 and PUB13, to associate with and polyubiquitinate FLS2 leading to flagellin-induced FLS2 degradation, and *pub12* and *pub13* mutants display elevated immune responses to flagellin treatment[26]. MYB30-interacting E3 ligase 1 (MIEL1) ubiquitinates transcription factor MYB30, leading to MYB30 degradation by proteasome and repression of the immune response[27,28]. When microbe-associated molecular patterns (MAMPs) are recognized, E3 ubiquitin ligase RING-H2 FINGER A3A (RHA3A) monoubiquitinates receptor-like cytoplasmic kinase BOTRYTIS-INDUCED KINASE 1 (BIK1), contributing to the release of BIK1 from the FLS2-BAK1 complex and activation of immune signaling[15].

Yield penalties usually accompany immune response activation[29,30]. Accordingly, plants have developed precise strategies to fine-tune immune responses for maintaining a low level of basal immunity under normal conditions but a rapid response upon pathogen infection. To minimize the fitness cost, plants employ different mechanisms to regulate the expression levels and stability of resistance-related proteins to an optimal level, including epigenetic regulation, miRNA-mediated regulation and proteasomal degradation. Moreover, creating pathogen-inducible transcriptional or translational control is also an effective way to enhance disease resistance without fitness cost[31–34].

Transcriptional reprogramming in response to a pathogen challenge is regulated by a broad variety of transcription factor families. Controlling the stability and transcriptional activity levels of transcription factors is necessary for plant immune response. Ideal Plant Architecture 1 (IPA1) was identified as an important transcription factor contributing to activation of plant immunity to *Magnaporthe oryzae* and the development of an ideal plant architecture that generates stronger panicles and higher yield[35–37]. Previous studies found that several candidates were involved in the IPA1 signaling pathway that modulates plant architecture[38] and established that the expression level and stability of IPA1 was essential for its function[6,39,40].

Although IPA1 phosphorylation that serves to quickly adjust IPA1 function was found to be a critical PTM induced by *M. oryzae* infection[37], we found that phosphorylation of IPA1 alone cannot directly activate the expression of immune response gene *WRKY45*. Therefore, there should be other co-activators serving to regulate IPA1 function in response to *M. oryzae* infection. In this study, we identified IPA1 interactor 7 (IPI7) as a coactivator for IPA1-mediated resistance to *M. oryzae*. IPI7, a RING-finger-containing E3 ligase, interacted with IPA1 and promoted the K29-polyubiquitination of IPA1 in vitro and in vivo. Although IPI7-mediated K29-polyubiquitination of IPA1 was induced by *M. oryzae* infection, the stability of IPA1 protein was not affected by IPI7. In vivo results indicated that IPI7-mediated K29-polyubiquitination was required for phosphorylated IPA1 to transactivate *WRKY45* expression for immune response activation, but not for plain IPA1 to transactivate *DEP1* expression for panicle development. Genetic evidence indicates that *IPI7*-knock out compromised IPA1-mediated resistance to *M. oryzae* but not panicle development. Our results reveal that ubiquitination mediated by IPI7 orchestrates with phosphorylation to control the transactivation activity of IPA1 for promoting plant immunity.

Results

Identification of IPA1-interacting protein IPI7

IPA1 protein becomes phosphorylated at its amino acid residue Ser163 upon *M. oryzae* infection, which serves to quickly adjust IPA1's function in activating the immune response. IPA1(S163D), which mimics IPA1 phosphorylated at Ser163, preferentially binds to the *WRKY45* promoter to activate downstream immune responses[37]. However, we found that IPA1(S163D) failed to activate *WRKY45* expression in tobacco leaves (Supplementary Fig. 1), indicating the requirement of other factors for IPA1 action on *WRKY45* expression.

To search for factors affecting IPA1 activity, we performed a yeast two-hybrid assay to screen for IPA1-interacting (IPI) proteins and tested their potential ability to coactivate *WRKY45* expression with IPA1(S163D) in tobacco leaf infiltration assays. We identified IPI7 that is capable of working with IPA1(S163D), but not with non-phosphorylated mutant IPA1, IPA1(S163A), to activate *WRKY45* expression (Supplementary Fig. 2). The interaction between IPI7 and IPA1 was then validated by in vitro and in vivo experiments including yeast-two hybrid (Fig. 1a), GST-pull down (Fig. 1b), bi-molecular fluorescence complementation (BiFC) (Fig. 1c) and co-immunoprecipitation (Co-IP) (Fig. 1d) assays.

IPA1 is ubiquitinated by IPI7

Sequence analysis revealed that IPI7 encodes a RING-finger-containing E3 ligase previously reported as APIP6[41]. We examined the E3 ligase activity of IPI7 and determined whether IPA1 is a substrate of IPI7. In in vitro ubiquitination assays, intact MBP-IPI7 showed E3 ligase activity and promoted polyubiquitination of His-TF-IPA1 in the presence of E1, E2 and ubiquitin proteins (Fig. 2a and Supplementary Fig. 3). However, MBP-IPI7(H58Y), carrying a mutation on histidine 58 in the RING finger domain, lost its E3 ligase activity and failed to promote the ubiquitination of IPA1 (Fig. 2a).

To confirm in vivo ubiquitination of IPA1 by IPI7, we co-expressed IPA1-HA and IPI7-MYC in tobacco leaves via *Agrobacterium tumefaciens* infiltration then immunoprecipitated IPA1 with an HA antibody, and found that stronger smear bands of ubiquitinated IPA1 were detected for IPA1-HA in the presence of IPI7-MYC (Supplementary Fig. 4). We then generated *IPI7*-overexpressing (*IPI7-OE*) transgenic plants in rice variety Ri22 (Supplementary Fig. 5a), which carries the *ipa1-1D* allele that contains a point mutation in the miR156 target site resulting in a

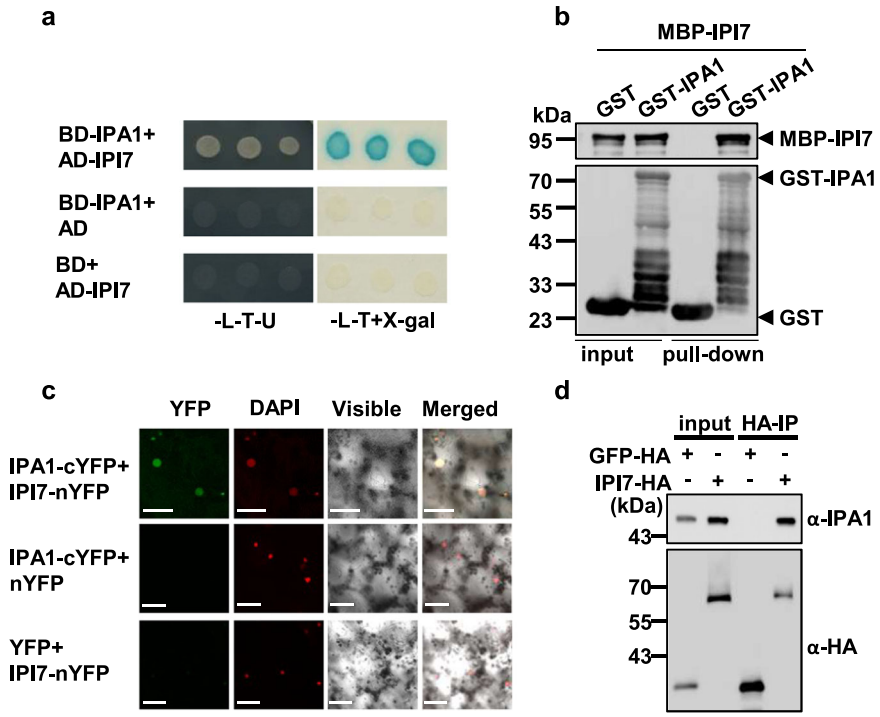

Fig. 1 | IPI7 interacts with IPA1. a Interaction between IPI7 and IPA1 in the yeast two-hybrid assay. IPA1 protein was fused with the GAL4 binding domain to generate BD-IPA1, and IPI7 with the GAL4 activation domain to form AD-IPI7. Blue clones in an X-Gal assay and clones grown on the SD-L-T-U medium indicate protein interaction in yeast cells. **b** GST pull-down assay for interaction between IPI7 and IPA1. MBP-IPI7, but not MBP, was pulled down with GST-IPA1 immobilized on glutathione-agarose beads. The immunoblot was probed separately with MBP and GST antibodies. Similar results were obtained from three independent biological experiments. **c** BiFC assay for interaction between IPI7 and IPA1 in tobacco leaves. IPA1 was fused with cYFP (C terminus of YFP) and IPI7 with nYFP (N terminus of YFP). Yellow fluorescence indicates interaction between IPI7 and IPA1 in the nucleus. DAPI was used as the nuclear marker. Bars = 10 μm. Similar results are obtained from three independent biological experiments. **d** IPI7 interacts with IPA1 in vivo. Total proteins from the protoplasts expressing IPI7-HA or GFP-HA were IP'd with a HA antibody. Proteins before (input) and after IP were detected with an antibody against IPA1 or HA. Similar results are obtained from two independent biological experiments.

higher level of IPA1 protein[35]. We detected a higher IPA1 ubiquitination level in the *IPI7-OE* plants than in Ri22 plants (Fig. 2b). These results indicate that IPI7 targets IPA1 for polyubiquitination.

The stability of IPA1 protein is not affected by IPI7

To test whether IPI7 affects IPA1 protein stability, we firstly co-expressed IPA1-HA and IPI7-MYC in tobacco leaves (Fig. 3a–c) or rice protoplast cells (Fig. 3d, e). Similar results indicated that the IPA1 protein level was stable with increased levels of IPI7-MYC protein. Then, we employed the CRISPR/Cas9 technology using two independent guide RNAs that target two different regions in the *IPI7* coding sequence to generate *IPI7*-knockout (*ipi7-ko*) transgenic plants in the Nipponbare (NP) rice genetic background and confirmed the mutations (Supplementary Fig. 6). We found no significant differences in IPA1 protein levels between *ipi7-ko* and wild-type NP plants (Fig. 3f and Supplementary Fig. 7a, b). Similar results were obtained in *IPI7* RNA interference (RNAi) plants where the IPA1 RNA level and protein level remained stable when *IPI7* expression was reduced by RNAi (*IPI7*-Ri) (Supplementary Fig. 7c–f).

Similarly, we found that IPA1 protein levels did not significantly alter in *IPI7-OE* transgenic plants compared to wild-type Ri22 (Fig. 3g and Supplementary Fig. 7g, h). These results suggest that the ubiquitination of IPA1 mediated by IPI7 does not lead to protein degradation, but may serve other purposes biochemically.

Ubiquitination mediated by IPI7 contributes to the transactivation of *WRKY45* by IPA1(S163D)

To further validate that IPI7 is a co-activator in IPA1(S163D)-mediated transactivation of *WRKY45*, we firstly examined the interaction between IPA1(S163D) and IPI7 and found that the phosphorylation mimic of IPA1 on Ser163 did not change the interaction between IPA1 and IPI7 (Supplementary Fig. 8a). Next, we performed in vivo and in vitro ubiquitination assays to compare the polyubiquitination levels of IPA1, IPA1(S163A) and IPA(S163D) mediated by IPI7 and found that there were no significant differences (Supplementary Fig. 8b, c). As expected, the stability of IPA1(S163D) protein was also not affected by IPI7 (Supplementary Fig. 8d).

Then, we tested whether IPI7 could help IPA1(S163D) to transactivate the *WRKY45* promoter fused to a *luciferase* (*LUC*) reporter in tobacco leaves. As shown in Fig. 4a, we detected significant light signals derived from *proWRKY45*:LUC only when co-expressed with both IPA1(S163D)-HA and IPI7-MYC, but not with IPA1(S163A) and IPI7-MYC (Fig. 4a and Supplementary Fig. 9). In rice protoplasts, we also found that IPI7 enhanced the effect of IPA1(S163D) to synergistically activate *proWRKY45*:LUC expression by nearly thirty-fold (Fig. 4b). However, IPI7(H58Y) lost nearly all its activity to enhance the transactivation activity of IPA1(S163D) on the *WRKY45* promoter in tobacco leaves and rice protoplasts (Fig. 4a, b), suggesting that the E3 ligase activity of IPI7 is essential for its function in promoting the transactivation activity of IPA1(S163D). In agreement, *ipi7-ko1* and *ipi7-ko2* plants expressed significantly lower *WRKY45* RNA levels than NP plants (Fig. 4c). These results indicate that ubiquitination of IPA1(S163D) mediated by IPI7 is required for IPA1(S163D) to activate *WRKY45* expression.

Our previous study indicated that phosphorylation of IPA1 at amino acid Ser163 alters the DNA binding specificity of IPA1, leading to a switch in target genes for IPA1 and IPA1(S163D)[37]. Thus, we tested the effects of IPI7 on the target-selection and transactivation specificity of IPA1 and found that addition of IPI7 has no effects on the activity of

https://doi.org/10.1038/s41467-024-51962-x

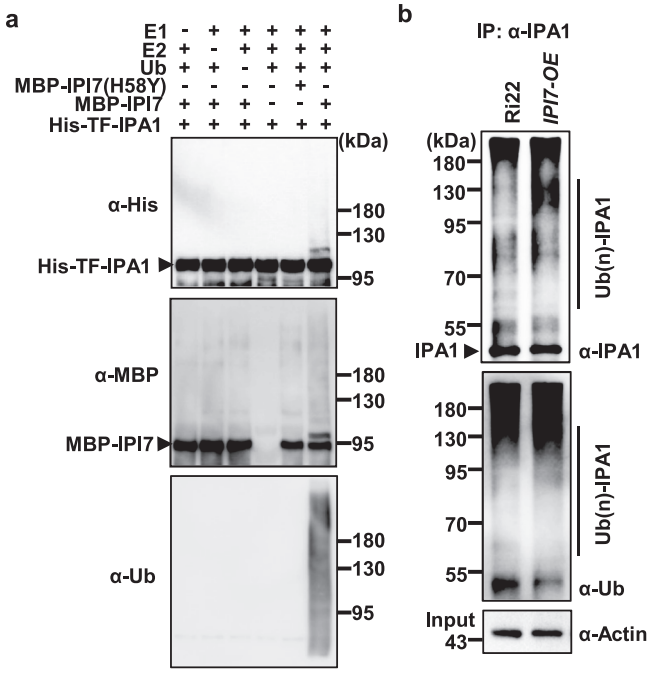

Fig. 2 | IPI7 ubiquitinates IPA1. a In vitro ubiquitination of His-IPA1 by MBP-IPI7. MBP-IPI7(H58Y) and MBP were used as negative controls. Immunoblotting was performed with antibodies against His, MBP or Ub. The presence (+) or absence (−) of components in the reaction mixture was indicated. Similar results were obtained from three independent biological experiments. **b** IPI7 promotes ubiquitination of IPA1 in vivo. The assay was performed with rice variety Ri22 and Ri22-derived transgenic plants overexpressing *IPI7* driven by a rice ubiquitin promoter (*IPI7-OE*). Immunoprecipitation was performed with an IPA1 antibody and immunoblotting was performed with an antibody against Ub or IPA1. Similar results were obtained from three independent biological experiments.

IPA1 to transactivate the *DEP1* promoter (Supplementary Fig. 10), which was identified as one of the key targets for IPA1, but not for IPA1(S163D)[37,38]. These results suggest that IPI7 is essential for the transactivation activity of IPA1(S163D) but not IPA1.

K29-polyubiquitination of IPA1 promoted by IPI7 is enhanced by *M. oryzae* infection

Different types of ubiquitination are suggested to lead to different the fates for substrates. To examine the ubiquitin-chain type covalently added on IPA1 in vivo that is promoted by IPI7, we used ubiquitin-chain-specific antibodies, including anti-K6, anti-K11, anti-K27, anti-K29, anti-K33, anti-K48, and anti-K63, to detect them in immunoblot assays. Anti-K6, anti-K29, and anti-K48 detected clear bands, but only anti-K29 detected a clear reduction in *ipi7-ko* plants for the K29-mediated ubiquitination of IPA1 (Fig. 5a and Supplementary Fig. 11a). These results suggest that IPI7 specifically promotes K29-polyubiquitination on IPA1 in vivo.

M. oryzae infection induces IPA1 phosphorylation at Ser163, which is necessary for IPA1-mediated activation of *WRKY45*. Thus, we asked whether ubiquitination of IPA1 by IPI7 is also influenced by *M. oryzae* infection. We performed in vivo ubiquitination assays using wild-type rice leaves infected with *M. oryzae* and found that IPA1 ubiquitination was induced by *M. oryzae* infection (Fig. 5b left and middle panels). In particular, K29-ubiquitination of IPA1 started to accumulate at 3 h post-inoculation (hpi), peaked at 6 hpi, then subsided to near basal levels within 12 hpi (Supplementary Fig. 11b). Interestingly, this pattern largely coincides with IPA1 phosphorylation, which starts to accumulate at 3 hpi, peaks at 6 to 12 hpi, then subsides to near normal levels within 48 hpi[37]. We further found that this enhancement of ubiquitination was inhibited in *ipi7-ko* plants (Fig. 5c left and middle panels). These results indicate that IPI7 is required for the K29-polyubiquitination of IPA1 induced by *M. oryzae* infection.

Knockout of *IPI7* blocks IPA1(S163D)-triggered immunity and rescues yield penalty

Examination of blast disease resistance by inoculation with *M. oryzae* showed that *ipi7-ko1* and *ipi7-ko2* plants developed significantly larger lesions and elevated fungal biomass (2-3 fold) than wild-type plants, indicating that *ipi7-ko* plants are compromised in resistance to *M. oryzae* (Supplementary Fig. 12a, b).

Because IPA1 was identified as a transcription factor contributing to panicle development[35,36], we analyzed the panicle morphology of *ipi7-ko* plants. *ipi7-ko1* and *ipi7-ko2* plants showed no clear changes in panicle length, numbers of primary and secondary branches, or grains per panicle compared with wild-type plants (Supplementary Fig. 12c–g). Thus, our results suggest that IPI7 positively regulates plant immunity, but does not play a major role in panicle development.

To validate the genetic role of IPI7 in orchestrating phosphorylation and ubiquitination in IPA1-mediated disease resistance and yield, we generated transgenic plants over-expressing IPA1(S163D) in *IPI7* knockout genetic background (*SD-OE/ipi7-ko*) (Supplementary Fig. 13) and examined their disease resistance to *M. oryzae*. We found that *SD-OE/ipi7-ko* plants developed lesions twice as large as *SD-OE* plants and the same size as NP plants (Fig. 6a). Fungal biomass determined by DNA quantification confirmed that *SD-OE/ipi7-ko* leaves harbored significantly larger *M. oryzae* populations than *SD-OE* leaves, but similar amounts as NP leaves (Fig. 6b), indicating that *ipi7-ko* neutralizes the immunity-enhancing effect of *SD-OE*.

We also detected RNA levels of *WRKY45*, a validated target of IPA1(S163D). While *WRKY45* RNA levels were highly induced in *SD-OE* plants, they were clearly reduced in *SD-OE/ipi7-ko* plants to the same level as in wild-type plants (Fig. 6c). These results provide further evidence that the impairment of *IPI7* blocks IPA1(S163D)-triggered immunity by arresting *WRKY45* activation. Furthermore, the detrimental effects of the hyper immune response triggered by IPA1(S163D) on rice yield traits, including panicle morphology, panicle length, primary and secondary branch numbers, and grains per panicle, were clearly alleviated in *SD-OE/ipi7-ko* plants (Fig. 6d, e), suggesting that ubiquitination orchestrates with phosphorylation for proper immune responses lowering fitness cost of IPA1 activation (Fig. 7).

Discussion

Here, we discover that rice plants utilize non-proteolytic K29-ubiquitination that fine-tunes the transcriptional activator activity of IPA1 to promote immunity in plants (Fig. 7). Plain IPA1 prefers binding to yield-related gene promoters which contain the “GTAC” motif and activates their expression[38]. Upon *M. oryzae* infection, phosphorylation at S163 is a target switch device that helps IPA1 to alter binding to disease resistance-related gene promoters which contain the “TGGGCC” motif[37]; however, this binding itself is only required but not sufficient to activate plant immunity. Although the expression levels of *IPI7* were not significantly changed by *M. oryzae* infection (Supplementary Fig. 14), IPI7-mediated K29-polyubiquitination of IPA1 is clearly induced by *M. oryzae* infection and serves as a booster to ensure that Ser163-phosphorylated IPA1 targets and transactivates immune-related genes such as *WRKY45*. These two post-translational modifications (ubiquitination and phosphorylation) of IPA1 protein play crucial roles in activating plant immunity. Thus, ubiquitination orchestrates with phosphorylation to form multiple regulatory layers that keep IPA1 in a balance among four different states: plain IPA1, phosphorylated IPA1, ubiquitinated IPA1, and ubiquitinated and phosphorylated IPA1. Only the ubiquitinated and phosphorylated IPA1 is the “pathogen-activated” IPA1, which binds to and transactivates immune-related genes like *WRKY45* to enhance plant immunity against *M. oryzae*. Moreover, ubiquitinated but unphosphorylated IPA1 can

https://doi.org/10.1038/s41467-024-51962-x

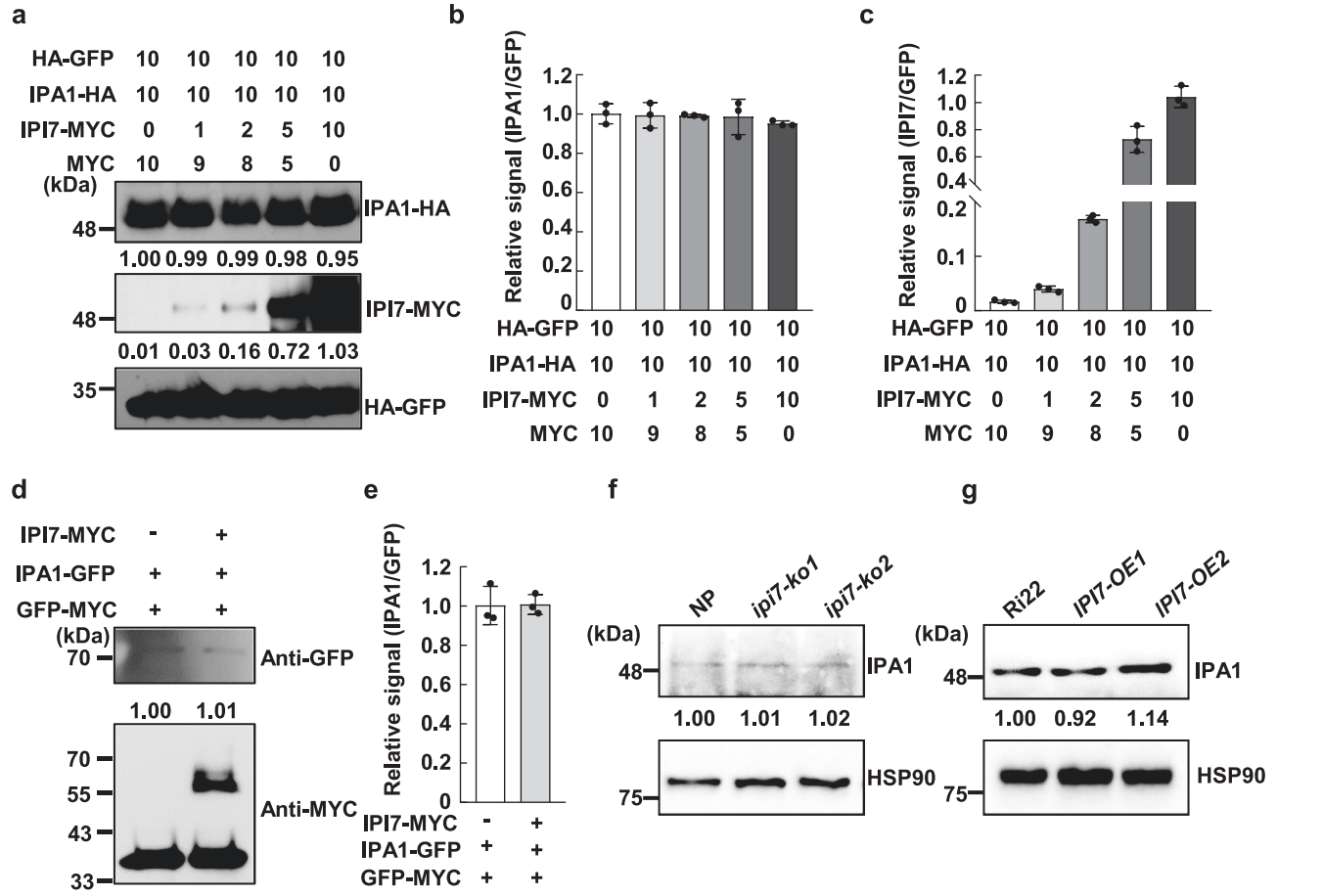

Fig. 3 | The stability of IPA1 protein is not affected by IPI7. a Stability of IPA1 protein with increasing levels of IPI7. Numbers indicate relative concentrations of *A. tumefaciens* carrying constructs used for co-infiltration. HA-GFP is an internal control for protein expression. Quantitation of protein bands of IPA1/GFP (**b**) and IPI7/GFP (**c**) for (**a**). Each value represents mean ± SD ($n = 3$ independent assays). **d** Stability of IPA1 with or without added IPI7 in rice protoplasts. The indicated plasmids were used to transfect rice protoplasts. IPA1-GFP protein amounts were quantitated by densitometry and normalized to the GFP-MYC level. **e** Statistical analysis of protein bands in (**d**) was conducted with three independent assays. Data are mean ± SD. IPA1 abundance in Nipponbare (NP), *ipi7-ko* plants (**f**), Ri22, and *IPI7-OE* plants (**g**). Samples were collected from indicated plants. IPA1 protein was probed in immunoblots with an IPA1 antibody and quantified by densitometry normalized to Heat Shock Protein 90 (HSP90). Similar results were obtained from three independent biological experiments in the dataset.

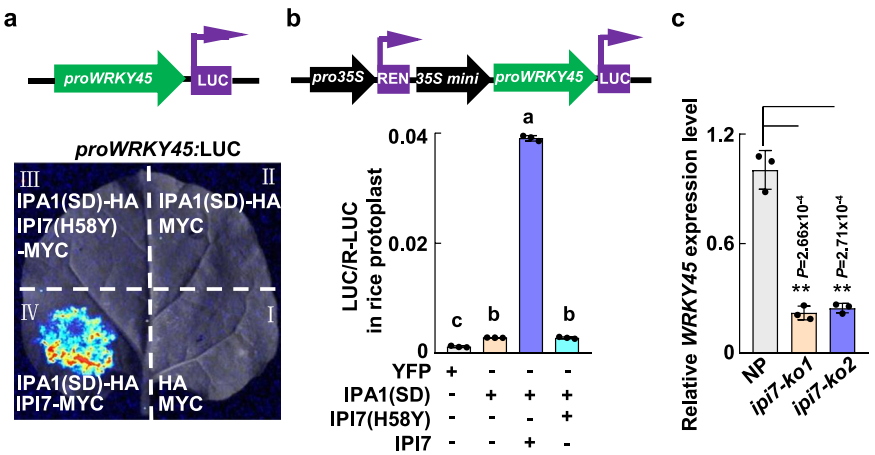

Fig. 4 | Ubiquitination of IPA1 mediated by IPI7 is essential for IPA1 to activate *WRKY45* expression. a, **b** Effects of IPA1(S163D) and IPI7 on transactivation of *WRKY45* promoter in tobacco leaves or rice protoplasts. **a** *A. tumefaciens* carrying plasmids were infiltrated into tobacco leaves. **b** Plasmids were used to transfect rice protoplasts. The luciferase (LUC) reporter is driven by the *WRKY45* promoter (*proWRKY45*:LUC); Renilla LUC was used as the internal reference. D-luciferin was applied as the LUC substrate. Each value represents mean ± SD ($n = 3$ independent biological samples). Different letters indicate significant differences determined by the Tukey–Kramer test, $p < 0.05$ (one-way ANOVA was conducted, followed by a two-sided honestly significant difference (HSD) test for multiple comparisons). *p* values are shown in the Source Data file. **c** *WRKY45* expression levels in NP and *ipi7-ko* plants were determined by RT-qPCR ($n = 3$ independent biological samples). ** indicates $p < 0.01$ (Two-tailed *t*-test for statistical analysis). Source data are provided as a Source Data file.

https://doi.org/10.1038/s41467-024-51962-x

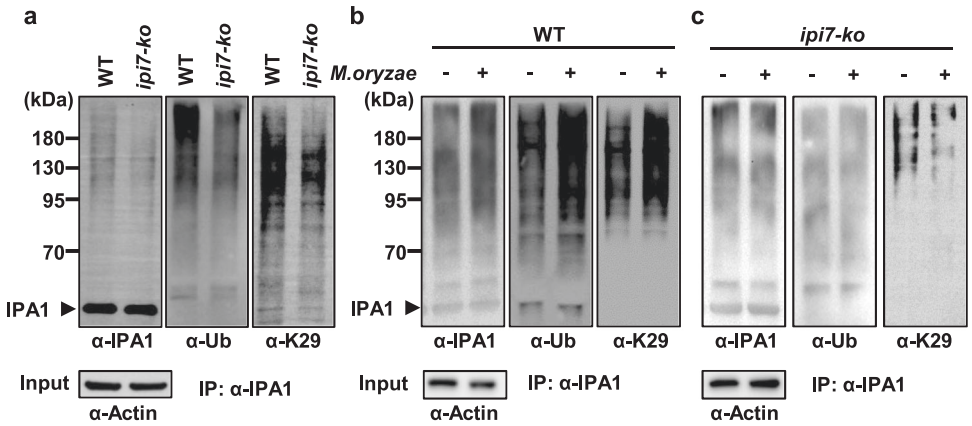

Fig. 5 | IPI7-mediated K29-polyubiquitination of IPA1 is induced by *M. oryzae*. **a** IPI7 is required for K29-polyubiquitination of IPA1. The assay was performed in wild-type plants and *ipi7-ko* plants. Immunoprecipitation was performed with an IPA1 antibody and immunoblotting was performed with an antibody against IPA1, Ub or K29-polyubiquitin chain (K29). Proteins before immunoprecipitation (input) were detected with an antibody against actin for normalization. Effects of *M. oryzae* infection on the ubiquitination of IPA1 in vivo in wild-type (**b**) and *ipi7-ko* (**c**) plants. Leaves were collected after inoculation with (+) or without (−) *M. oryzae*. Immunoprecipitation was performed with an IPA1 antibody and immunoblotting was performed with an antibody against IPA1, Ub or K29. Proteins before immunoprecipitation (input) were probed with an antibody against actin for normalization. Similar results were obtained from three independent biological experiments in the datasets.

also target growth-related genes for yield, which might compensate for the penalty caused by pathogen-activated IPA1. Therefore, these four states of IPA1 working together to build an effective system that timely enables IPA1 to promote both the immune response and yield in plants.

IPI7/APIP6 interacts with different proteins and targets them for ubiquitination. Previous studies indicated that IPI7/APIP6 targets Avr-Piz-t, OsELF3-2 and ROD1 for ubiquitination and promotes their degradation via the ubiquitin-proteasome system (UPS)[32,41,42]. Differently, our study found that ubiquitination of IPA1 mediated by IPI7 is not necessary for the degradation of IPA1 via the UPS (Fig. 3), but is critical for the transactivation of *WRKY45* by IPA1 in response to pathogen attack (Figs. 4 and 6). Moreover, we found that the ubiquitination of IPA1 mediated by IPI7 did not affect its binding to downstream target genes (Supplementary Fig. 15). These results suggest that the molecular mechanism of ubiquitination of IPA1 promoted by IPI7 is different from previous studies and the substrates labeled with polyubiquitin chains by IPI7 have different fates.

Polyubiquitin chains are formed through the linkage of lysine residues other than K48 of the ubiquitin molecule, i.e., K6-, K11-, K27-, K29-, K33- and K63-linked ubiquitination[43,44]. Accordingly, the abundance, function, activity and subcellular distribution of substrates involved in different cellular and physiological processes can be regulated through different types of ubiquitin modifications. Of these various types of polyubiquitination, the K48-linked ubiquitination is the best characterized one which usually serves to proteolytically degrade substrates. By contrast, other types of ubiquitination are much less well understood in plants. We tested the ubiquitin chain types on IPA1 promoted by IPI7 using different ubiquitin-chain-specific antibodies and found that the IPI7-mediated enhancement of K29-polyubiquitination of IPA1 is crucial for the IPA1-mediated response to *M. oryzae* (Figs. 5, 6 and Supplementary Fig. 11). Our results suggest that the K29-polyubiquitin chain modification is involved in plant immune response by regulating IPA1(S163D) activity. However, the transcriptional activation activities of plain IPA1 and IPA1(S163A) were unaffected by IPI7-mediated ubiquitination (Supplementary Figs. 9b and 10), which might be due to the differences in the 3D structures of plain IPA1, phosphorylated IPA1, ubiquitinated IPA1, phosphorylated and ubiquitinated IPA1.

E3 ligases play a crucial role in governing substrate specificity, while the E2 ubiquitin–conjugating enzyme is often considered as a "carrier of ubiquitin" determining the topology of the polyubiquitin chain[45]. E3 selects the right E2 to generate the appropriate Ub signal on the target protein, thus controlling the fate of a given substrate[46]. Therefore, different E2s may be selected by IPI7 to work together in different signaling pathways.

Ubiquitination is also named "lysine ubiquitination" for many years because it occurs when a ubiquitin or ubiquitin-chain is covalently attached to a lysine (K) residue of the targeted protein. Sequence analysis reveals that there are seven K residues in IPA1 protein. However, we found that none of the seven single-K-site disruptions in IPA1 affected IPI7-mediated ubiquitination (Supplementary Fig. 16). Recently, it has been established that cysteine, serine and threonine residues also function as sites for ubiquitination, forming thioester, hydroxyester and peptide bonds, respectively, dependent on the free amino group of the N-terminus of target protein[43]. Therefore, the ability of IPA1 to be ubiquitinated by IPI7 on more than one type of amino acids creates many regulatory possibilities.

Plant immune responses often penalize growth and yield. Crop varieties with enhanced disease resistance and low fitness cost are highly desired by breeders. The utilization of a pathogen-inducible transcriptional and/or translational control is an effective way to restrict expression of resistance genes at the most appropriate level[34,47]. For example, a TBF1 cassette was used to regulate expression of a resistance gene to enhance broad-spectrum disease resistance without compromising plant fitness[34]. Epigenetic modification built an accurate expression pattern for PigmR and PigmS in nature, leading to activation of PigmR-mediated defense response in leaves while allowing grain production in panicles[31]. These findings have led to useful strategies to balance yield and immunity in breeding programs by regulating the expression levels of resistance genes. Our results yield new insights into how crops can achieve high yield and disease resistance simultaneously. Various disease resistance-related proteins require ubiquitination, phosphorylation or other PTMs to initiate their activation processes. The employment of PTMs to monitor the activity of immune-related proteins is an effective way to minimize fitness cost.

Methods

Plant materials and growth conditions

Rice (*Oryza sativa*) *ssp japonica* cultivated variety Nipponbare (NP), Ri22, *ipi7-ko*, and *IPI7-OE* plants were grown either in the greenhouse or

https://doi.org/10.1038/s41467-024-51962-x

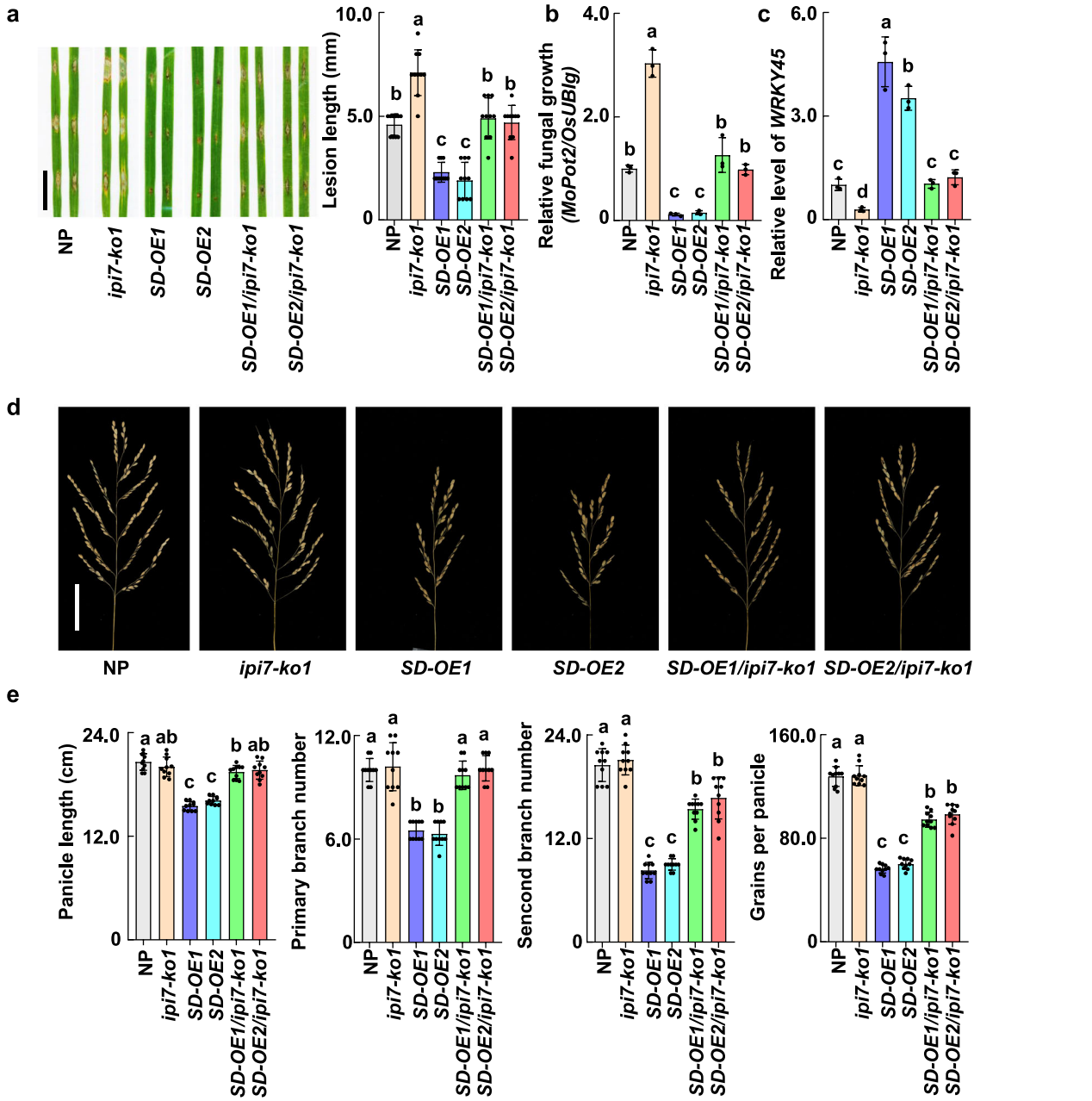

Fig. 6 | IPI7 contributes to IPA1-mediated disease resistance with lower fitness cost. a, **b** Effects of *IPI7* knockout on IPA1(S163D)-mediated resistance to *M. oryzae*. Rice leaves were punch-inoculated with *M. oryzae* and incubated for a week. Lesion pictures are displayed, and 10 independent lesion lengths are measured (right panel) (**a**), *M. oryzae* populations determined based on fungal *MoPot2* DNA content (**b**) are presented. Each value represents mean ± SD ($n = 3$ independent biological samples). **c** *WRKY45* RNA levels in the leaves of NP, *ipi7-ko*, *IPA1(S163D)* over-expression (*SD-OE*) and *SD-OE*/*ipi7-ko* double transgenic plants were determined by RT-qPCR ($n = 3$ independent biological samples). **d** Main panicle morphology of NP, *ipi7-ko1*, *SD-OE*, and *SD-OE/ipi7-ko* plants. Scale bar = 5 cm. **e** Statistical analysis of main panicle length, primary and secondary branch numbers, and grains per main panicle of NP and different transgenic plants. Each value represents mean ± SD ($n = 10$ rice plants). Different letters indicate significant differences at $p < 0.05$ (one-way ANOVA was conducted, followed by two-sided HSD test for multiple comparisons). The corresponding p values can be found in the Source Data. Source data are provided as a Source Data file.

experimental fields of the Sichuan Agricultural University (Chengdu, Sichuan, China).

The *ipi7-ko* plants were generated using CRISPR/Cas9 carried out by Biogle.cn. To minimize the potential off-target effects induced by CRISPR/Cas9, we performed two distinct transformations, using two sgRNAs targeting *IPI7* at different locations: SG1 (TGCTGTATCTTC TGCACCTG) and SG2 (AGCTCATCCATGCCCATATG) (Supplementary Fig. 6). Individual sgRNA construct was created in the BGK03 vector containing Cas9, introduced into *Agrobacterium tumefaciens* strain EHA105, and transformed into NP. Six independent lines for each of SG1 and SG2 were obtained. To examine the CRISPR/Cas9-created lines, genomic DNA was extracted from transgenic plants and primer pairs flanking the designed target site were used for PCR amplification (Supplementary Data 1). Sequence alignment revealed that two independent mutants, *ipi7-ko1* and *ipi7-ko2*, were obtained (Supplementary Fig. 6).

The *Ubi-IPI7* and *35S*:Flag-IPA1(S163D) plasmids were individually introduced into *A. tumefaciens* strain EHA105 and transformed into

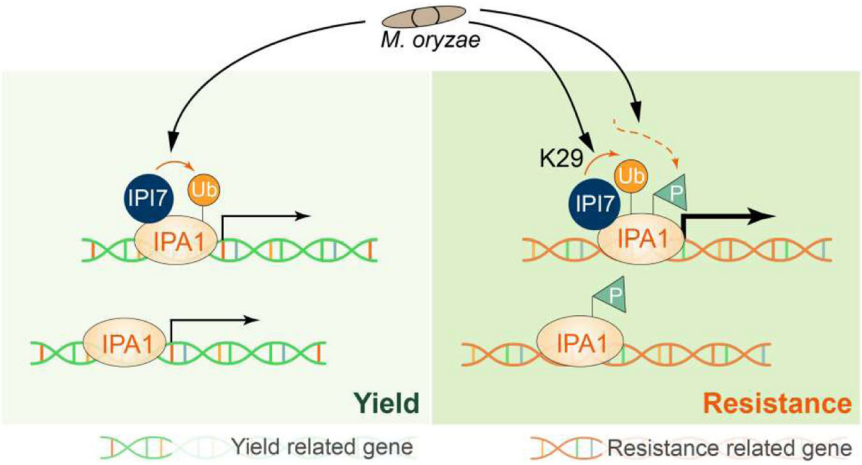

Fig. 7 | A PTMs-monitoring model in which IPA1 promotes grain yield and disease resistance to *M. oryzae*. Under normal conditions, IPA1 activates the promoters of various yield-related genes, promoting plant growth and yield. Upon *M. oryzae* challenge, IPA1 goes through four statuses: plain IPA1, ubiquitinated IPA1, phosphorylated IPA1, and ubiquitinated and phosphorylated IPA1. First, both plain IPA1 and ubiquitinated IPA1 promote expression of yield-related genes to increase grain yield. Second, phosphorylated IPA1 binds to promoters of the immune-related genes, including *WRKY45* promoter, without transactivation activity. Third, ubiquitinated and phosphorylated IPA1, which represents "blast-activated" IPA1, binds to and transactivates immune-related genes to enhance host resistance to *M. oryzae*.

Ri22, NP or *ipi7-ko* plants as previously reported[48]. Independent lines with increased expression of *IPI7* or *IPA1* were obtained and used in further investigation.

Constructs

In brief, target fragments were generated by PCR amplification using primers listed in Supplementary Data 1. The linearized vector terminal 15–20 bp sequence was used as homologous sequence and added to the 5′ end of the gene-specific positive/reverse amplification primer sequences. The insert fragments with homologous sequence were ligated into desired vectors or cloned into desired vectors using ClonExpress® II One Step Cloning Kit (Vazyme, C112-01). The vectors used in the yeast two-hybrid assay were pDBLeu for bait and pPC86 for prey. pSPYCE and pSPYNE vectors were used for the BiFC assay[49]. The coding regions of targets were inserted into the pGEX-6P-1, pMAL-c2x or pCold™-TF (TaKaRa, Cat# 3365) vector for protein expression in vitro. The promoters of *DEP1* and *WRKY45* were amplified from NP genomic DNA and ligated into the pCAMBIA1300-LUC vector to produce *proDEP1*:LUC and *proWRKY45*:LUC, respectively. Point mutation constructs were generated with the Quikchange site-directed mutagenesis kit (Stratagene, 200514). All of the primers used in constructs are listed in Supplementary Data 1.

Yeast Two-Hybrid assay

Yeast Two-Hybrid assay was performed as previously reported[8]. Plasmids were co-transferred into the MAV203 yeast strain, and transformed cells were grown on SD medium without Leu and Trp. The clones were then confirmed by growing on SD medium without Leu, Trp, and Ura for 2 days, or using X-gal assay.

Protein expression in vitro

GST-, MBP-, and His-fused proteins were individually expressed in Transetta(DE3) cells (TransGen Biotech, CD801). GST-fused proteins were purified using glutathione-conjugated Sepharose 4 Fast Flow (Sangon Biotech, 17-5132-01); the MBP-fused proteins were purified using Amylose Resin (Sangon Biotech, C500096-0005); the His-fused proteins were purified using Ni-Sepharose 6 Fast Flow (Sangon Biotech, C600033-002), according to manufacturer's instructions.

Pull-down assay

Pull down assay was performed according to a previously described method[50] with some modifications. Approximately 10 μg of GST or GST-IPA1 were incubated with 5 μL of prewashed glutathione agarose beads in 1 mL of pull-down buffer (20 mM Tris-HCl, PH 7.5, 1 mM β-mercaptoethanol, 3 mM EDTA, 1 mM DTT, 1% [v/v] Nonidet P-40, 1× Protease Inhibitor Cocktail, Beyotime) for 1 h at 4 °C with gentle shaking. The beads were harvested by centrifugation at 150 × *g* for 1 min, then mixed with 10 μg of MBP-IPI7 in 1 mL of pull-down buffer for 2 h at 4 °C with gentle shaking. Finally, the beads were harvested and washed three times with 1 mL of pull-down buffer and once more with 1 mL of 50 mM Tris-HCl, pH 7.5. The proteins pulled down were released from beads by boiling in SDS-PAGE sample loading buffer and analyzed by immunoblotting with a GST (Thermo Fisher Scientific MA4-004) or MBP antibody (NEW ENGLAND BioLabs, E8032S).

Transient expression, BiFC and transactivational activity assay

Transient expression assay was performed as previously reported[51]. Leaves of 4 weeks old *N. benthamiana* were infiltrated with *A. tumefaciens* carrying test constructs. In all cases, cultures were co-infiltrated with *A. tumefaciens* carrying a P19 suppressor in a gene silencing construct.

BiFC assay was performed in *N. benthamiana* leaves. *N. benthamiana* leaves were infiltrated with *A. tumefaciens* carrying constructs in the pSPYCE vector. Two days after infiltration, visible signals were examined under a confocal microscope (NiKon A1 i90, LSCM, Japan).

Transactivational activity assay was carried out in an *Agrobacterium*-mediated transient expression system. *N. benthamiana* leaves were infiltrated with *A. tumefaciens* carrying a *proDEP1*:LUC or *proWRKY45*:LUC reporter construct, together with *A. tumefaciens* carrying an IPA1(SD)-HA or IPA1-HA construct, and *A. tumefaciens* carrying an IPI7-MYC or IPI7(H58Y)-MYC construct. 60 h after infiltration, detached leaves were sprayed with 1 mM D-luciferin, potassium salt (Invitrogen™Abcam, 115144-35-9) following manufacturer's instructions. The Renilla *LUC* gene under control of the CaMV 35S promoter was co-transferred as an internal control. Luminescence signals were captured using a charge-coupled device (CCD) camera (BIO-RAD, ChemiDocTM Touch Imaging System). Then the luciferase activities were calculated using the Dual Luciferase Reporter Gene Assay Kit

(Beyotime, RG027) according to manufacturer's instructions. The ratio of LUC activities (firefly LUC/Renilla LUC) was calculated to normalize each assay.

In vitro ubiquitination assay

Ubiquitination assay was performed as previously described[8] with some modifications: 1 μg GST-IPI7 or GST protein was incubated in a 20 μL reaction mixture containing 50 mM Tris-HCl, pH 7.5, 5 mM $MgCl_2$, 2 mM DTT, 5 mM ATP, 3 mM creatine phosphate (Solarbio, 922-32-7), 1 unit creatine kinase (Roche 10127566001), 100 ng E1 (Boston Biochem, E-305), 100 ng E2 (Boston Biochem, E2-607), and 4 μg ubiquitin (Boston Biochem, U-100). To confirm IPI7-mediated ubiquitination of IPA1, purified His-IPA1 protein (2 μg) was added to the reaction mixture and incubated at 30 °C for 1.5 h. The reaction was stopped by adding 5× SDS sample buffer and boiling at 100 °C for 10 min. The protein mixture was then separated in a 10% (w/v) SDS-PAGE.

In vivo ubiquitination assay

In vivo ubiquitination of IPA1 protein was performed as previously described[8] with some modifications. Briefly, samples were ground into powder in liquid nitrogen and extracted in protein extraction buffer NB1 containing 50 mM Tris-MES (pH 8.0), 0.5 M sucrose, 1 mM $MgCl_2$, 10 mM EDTA, 5 mM DTT (Solarbio, D8220), and 1× Protease Inhibitor Cocktail (APEXBIO, K1008). The crude extracts containing 500 μg protein were co-incubated with IPA1 polyclonal antibodies and 50 μM MG132 (Selleck.cn, S2619). After gentle shaking for 1 h, 30 μL Pierce™ Protein A/G Magnetic beads (Thermo Fisher Scientific, 88802) were added into the mixture and incubated for another 1 h with gentle shaking. The magnetic beads were washed with NB1 buffer for 3 times. After an equal volume of 2× SDS buffer was added and boiled at 100 °C for 10 min, the sample was run on a 10% (w/v) SDS-PAGE, immunoblotted, and probed with IPA1, ubiquitin (Beyotime, AF1705), and 7 different Ub chain-specific antibodies. Detailed information for the 7 Ub chain-specific antibodies can be found at the company website (https://abclonal.com.cn; https://www.bio-swamp.com) with the following catalog numbers: anti-K6 (Abclonal, A18106); anti-K11 (Bioswamp, PAB46885); anti-K27 (Abclonal, A18202); anti-K29 (Abclonal, A18198); anti-K33 (Abclonal, A18199); anti-K48 (Abclonal, A3606); anti-K63 (Abclonal, A18164).

Ubiquitination combined with electrophoretic mobility shift assay

Firstly, an in vitro ubiquitination assay was performed as described before. Then, an EMSA assay was performed to detect the DNA binding activity of IPA1(S163D) protein in the in vitro ubiquitination assay reactions. Six μL products from the in vitro ubiquitination assay were incubated with single-biotin-labeled DNA probes of *WRKY45* promoter for the EMSA assay[37]. Light Shift Chemiluminescent EMSA Kit (Beyotime, GS009) was used for detection in the EMSA assay. Detailed EMSA procedure followed manufacturer's instructions. Photos were taken using a charge-coupled device (CCD) camera.

RNA extraction and reverse transcription quantitative PCR (RT-qPCR)

Total RNA was prepared with a TRIzol Kit (Thermo Fisher Scientific, 15596-018CN) according to user's manual. cDNAs were generated using the PrimeScript RT Reagent Kit with gDNA Eraser (Perfect Real Time) (TaKaRa, Cat# RR047A). RT-qPCR was performed following the manufacturer's instructions in the QuantiNova SYBR Green PCR Kit (QIAGEN, Cat# 208054). The primers used in RT-qPCR are listed in Supplementary Data 1. *Ubiquitin* (LOC_Os03g13170) was used as the internal control for normalization.

M. oryzae inoculation assay and protein extraction

For pathogen infection, a punch inoculation assay was carried out on rice leaf strips from 4-week-old plants as previously described[52]. Lesion size was measured after incubation for 5–7 days at 28 °C. Genomic DNA was isolated to measure the *Pot2* gene of *M. oryzae* and calculated relative to a rice *ubiquitin* gene for normalization.

Leaves detached from 4-week-old plants were cut into 4-cm-long strips and incubated for 12 h in H_2O to reduce residual wounding effects before further treatment. The leaf strips were treated with or without blast isolate ZHONG10-8-14 with a final concentration of 5×10^5 conidia/mL. Treated or non-treated samples were collected and ground into powder in liquid nitrogen and resuspended in NB1 buffer [50 mM 2-amino-2-(hydroxymethyl)−1,3-propanediol (TRIS)-MES pH 8.0, 0.5 M sucrose, 1 mM $MgCl_2$, 10 mM EDTA, 1× Protease Inhibitor Cocktail (APExBio, K1008), 5 mM DTT (Solarbio, D8220)] on ice. Extracts were centrifuged at 13,000 × *g* at 4 °C for 10 min, and the supernatant was boiled at 100 °C for 10 min after adding 5× SDS buffer. The sample was run on a 10% (w/v) SDS-PAGE, immunoblotted, and probed with an IPA1 antibody. The protein level of actin was used as an internal control (Sangon Biotech, NO. D191048).

Western blots and analysis

Samples were boiled for 10 min and centrifuged at 11,000 × *g* for 2 min at room temperature. A total of 10–20 μL samples were loaded in an 8% or 10% SDS-PAGE gel. After electrophoresis, the proteins were transferred to a PVDF membrane using the TransBlot Turbo Transfer System (Bio-Rad, USA). The membranes were blocked with 4% non-fat milk in Tris-buffered saline with Tween 20 (TBST, containing 20 mM Tris, pH 7.6, 150 mM NaCl, 0.1% Tween 20) at room temperature for 2 h and then incubated overnight with a primary antibody at 4 °C. The primary antibodies were used in this study along with appropriate secondary antibody-HRP conjugates. The information of antibodies used is as indicated. Protein bands were visualized using an ECL chemiluminescence detection kit (Sangon, China, No. C500044), and they were imaged using a chemiluminescence imaging system (Bio-Rad, USA). The relative protein intensity was analyzed using ImageJ.

Statistics and reproducibility

Fluorescence images are collected using a Nikon A1 i90 LSCM confocal microscope. The ChemiDocTM Touch Imaging System from Bio-Rad is used for collecting protein images and Dul-Luciferase reporter images, while the ImageJ software is utilized for quantitative analysis of protein bands. The experimental data of the Dul-Luciferase reporter were collected using GLOMAXTM96. GraphPad 8.0 was used for all data analysis. The statistical analyses were conducted using SPSS 21.0. All values are presented as mean ± SD, and the number (n) of samples is indicated in the figure legend. Statistically significant differences between the control and experimental groups were determined using a one-way ANOVA with a two-sided honestly significant difference (HSD) multiple comparison test or t-test. Differences were considered statistically significant when the p value is <0.05. All experiments were repeated at least twice, and multiple biological replicates were used in each experiment. No data was excluded from the analyses. The investigators were not blinded to the allocation during experiments or outcome assessment.

Reporting summary

Further information on research design is available in the Nature Portfolio Reporting Summary linked to this article.

Data availability

All data are available in the main text and the Supplementary Information. Source data are provided with this paper.

References

1. Jones, J. D. & Dangl, J. L. The plant immune system. *Nature* **444**, 323–329 (2006).
2. Veronese, P. et al. The membrane-anchored BOTRYTIS-INDUCED KINASE1 plays distinct roles in Arabidopsis resistance to necrotrophic and biotrophic pathogens. *Plant Cell* **18**, 257–273 (2006).
3. Nürnberger, T., Brunner, F., Kemmerling, B. & Piater, L. Innate immunity in plants and animals: striking similarities and obvious differences. *Immunol. Rev.* **198**, 249–266 (2004).
4. Liu, L. J. et al. COP1-mediated ubiquitination of CONSTANS is implicated in cryptochrome regulation of flowering in Arabidopsis. *Plant Cell* **20**, 292–306 (2008).
5. Martins, S. et al. Internalization and vacuolar targeting of the brassinosteroid hormone receptor BRI1 are regulated by ubiquitination. *Nat. Commun.* **6**, 6151 (2015).
6. Miao, Y. & Zentgraf, U. A HECT E3 ubiquitin ligase negatively regulates Arabidopsis leaf senescence through degradation of the transcription factor WRKY53. *Plant J.* **63**, 179–188 (2010).
7. Mithoe, S. C. & Menke, F. L. Regulation of pattern recognition receptor signalling by phosphorylation and ubiquitination. *Curr. Opin. Plant. Biol.* **45**, 162–170 (2018).
8. Wang, J. et al. Tissue-specific ubiquitination by IPA1 INTERACTING PROTEIN1 modulates IPA1 protein levels to regulate plant architecture in rice. *Plant Cell* **29**, 697–707 (2017).
9. Wang, L. et al. Strigolactone signaling in arabidopsis regulates shoot development by targeting D53-like SMXL repressor proteins for ubiquitination and degradation. *Plant Cell* **27**, 3128–3142 (2015).
10. Xu, Y. et al. UBIQUITIN-SPECIFIC PROTEASE14 interacts with ULTRAVIOLET-B INSENSITIVE4 to regulate endoreduplication and cell and organ growth in arabidopsis. *Plant Cell* **28**, 1200–1214 (2016).
11. Ciechanover, A. & Schwartz, A. L. The ubiquitin-proteasome pathway: the complexity and myriad functions of proteins death. *Proc. Natl. Acad. Sci. USA* **95**, 2727–2730 (1998).
12. Sadowski, M., Suryadinata, R., Tan, A. R., Roesley, S. N. & Sarcevic, B. Protein monoubiquitination and polyubiquitination generate structural diversity to control distinct biological processes. *IUBMB Life* **64**, 136–142 (2012).
13. Braten, O. et al. Numerous proteins with unique characteristics are degraded by the 26S proteasome following monoubiquitination. *Proc. Natl. Acad. Sci. USA* **113**, E4639–E4647 (2016).
14. Gu, X., Jiang, D., Wang, Y., Bachmair, A. & He, Y. Repression of the floral transition via histone H2B monoubiquitination. *Plant J.* **57**, 522–533 (2009).
15. Ma, X. et al. Ligand-induced monoubiquitination of BIK1 regulates plant immunity. *Nature* **581**, 199–203 (2020).
16. Pickart, C. M. & Fushman, D. Polyubiquitin chains: polymeric protein signals. *Curr. Opin. Chem. Biol.* **8**, 610–616 (2004).
17. Leitner, J. et al. Lysine63-linked ubiquitylation of PIN2 auxin carrier protein governs hormonally controlled adaptation of Arabidopsis root growth. *Proc. Natl. Acad. Sci. USA* **109**, 8322–8327 (2012).
18. Vierstra, R. D. The ubiquitin-26S proteasome system at the nexus of plant biology. *Nat. Rev. Mol. Cell Biol.* **10**, 385–397 (2009).
19. Yin, J., Yi, H., Chen, X. & Wang, J. Post-translational modifications of proteins have versatile roles in regulating plant immune responses. *Int. J. Mol. Sci.* **20**, 2807 (2019).
20. Chen, H. et al. A bacterial type III effector targets the master regulator of salicylic acid signaling, NPR1, to subvert plant immunity. *Cell Host Microbe* **22**, 777–788.e777 (2017).
21. Gimenez-Ibanez, S. et al. AvrPtoB targets the LysM receptor kinase CERK1 to promote bacterial virulence on plants. *Curr. Biol.* **19**, 423–429 (2009).
22. Göhre, V. et al. Plant pattern-recognition receptor FLS2 is directed for degradation by the bacterial ubiquitin ligase AvrPtoB. *Curr. Biol.* **18**, 1824–1832 (2008).
23. Popov, G., Majhi, B. B. & Sessa, G. Effector gene xopAE of Xanthomonas euvesicatoria 85-10 is part of an operon and encodes an E3 ubiquitin ligase. *J. Bacteriol.* **200**, e00104–e00118 (2018).
24. Qin, J. et al. The Xanthomonas effector XopK harbours E3 ubiquitin-ligase activity that is required for virulence. *New. Phytol.* **220**, 219–231 (2018).
25. Shan, L. et al. Bacterial effectors target the common signaling partner BAK1 to disrupt multiple MAMP receptor-signaling complexes and impede plant immunity. *Cell Host Microbe* **4**, 17–27 (2008).
26. Lu, D. et al. Direct ubiquitination of pattern recognition receptor FLS2 attenuates plant innate immunity. *Science* **332**, 1439–1442 (2011).
27. Marino, D. et al. Arabidopsis ubiquitin ligase MIEL1 mediates degradation of the transcription factor MYB30 weakening plant defence. *Nat. Commun.* **4**, 1476 (2013).
28. Marino, D. et al. Addendum: Arabidopsis ubiquitin ligase MIEL1 mediates degradation of the transcription factor MYB30 weakening plant defence. *Nat. Commun.* **10**, 1475 (2019).
29. Brown, J. K. A cost of disease resistance: paradigm or peculiarity? *Trends Genet.* **19**, 667–671 (2003).
30. Bergelson, J. & Purrington, C. B. Surveying patterns in the cost ofresistance in plants. *Am. Nat.* **148**, 536–558 (1996).
31. Deng, Y. et al. Epigenetic regulation of antagonistic receptors confers rice blast resistance with yield balance. *Science* **355**, 962–965 (2017).
32. Gao, M. et al. Ca(2+) sensor-mediated ROS scavenging suppresses rice immunity and is exploited by a fungal effector. *Cell* **184**, 5391–5404.e5317 (2021).
33. Wang, H. et al. Suppression of rice miR168 improves yield, flowering time and immunity. *Nat. Plants* **7**, 129–136 (2021).
34. Xu, G. et al. uORF-mediated translation allows engineered plant disease resistance without fitness costs. *Nature* **545**, 491–494 (2017).
35. Jiao, Y. et al. Regulation of OsSPL14 by OsmiR156 defines ideal plant architecture in rice. *Nat. Genet.* **42**, 541–544 (2010).
36. Miura, K. et al. OsSPL14 promotes panicle branching and higher grain productivity in rice. *Nat. Genet.* **42**, 545–549 (2010).
37. Wang, J. et al. A single transcription factor promotes both yield and immunity in rice. *Science* **361**, 1026–1028 (2018).
38. Lu, Z. et al. Genome-wide binding analysis of the transcription activator ideal plant architecture1 reveals a complex network regulating rice plant architecture. *Plant Cell* **25**, 3743–3759 (2013).
39. Song, X. et al. Targeting a gene regulatory element enhances rice grain yield by decoupling panicle number and size. *Nat. Biotechnol.* **40**, 1403–1411 (2022).
40. Zhang, L. et al. A natural tandem array alleviates epigenetic repression of IPA1 and leads to superior yielding rice. *Nat. Commun.* **8**, 14789 (2017).
41. Park, C. H. et al. The Magnaporthe oryzae effector AvrPiz-t targets the RING E3 ubiquitin ligase APIP6 to suppress pathogen-associated molecular pattern-triggered immunity in rice. *Plant Cell* **24**, 4748–4762 (2012).
42. Ning, Y. et al. OsELF3-2, an ortholog of Arabidopsis ELF3, interacts with the E3 ligase APIP6 and negatively regulates immunity against Magnaporthe oryzae in rice. *Mol. Plant* **8**, 1679–1682 (2015).
43. McDowell, G. S. & Philpott, A. New insights into the role of ubiquitylation of proteins. *Int. Rev. Cell. Mol. Biol.* **325**, 35–88 (2016).
44. Yau, R. & Rape, M. The increasing complexity of the ubiquitin code. *Nat. Cell Biol.* **18**, 579–586 (2016).
45. Nakamura, N. Ubiquitin system. *Int. J. Mol. Sci.* **19**, 1080 (2018).
46. Cook, B. W., Lacoursiere, R. E. & Shaw, G. S. Recruitment of ubiquitin within an E2 chain elongation complex. *Biophys. J.* **118**, 1679–1689 (2020).

47. Liu, M. et al. Inducible overexpression of ideal plant architecture1 improves both yield and disease resistance in rice. *Nat. Plants* **5**, 389–400 (2019).
48. Hiei, Y., Ohta, S., Komari, T. & Kumashiro, T. Efficient transformation of rice (Oryza sativa L.) mediated by Agrobacterium and sequence analysis of the boundaries of the T-DNA. *Plant J.* **6**, 271–282 (1994).
49. Waadt, R. et al. Multicolor bimolecular fluorescence complementation reveals simultaneous formation of alternative CBL/CIPK complexes in planta. *Plant J.* **56**, 505–516 (2008).
50. Zhou, J. et al. Differential phosphorylation of the transcription factor WRKY33 by the protein kinases CPK5/CPK6 and MPK3/MPK6 cooperatively regulates camalexin biosynthesis in arabidopsis. *Plant Cell* **32**, 2621–2638 (2020).
51. Liu, L. et al. An efficient system to detect protein ubiquitination by agroinfiltration in Nicotiana benthamiana. *Plant J.* **61**, 893–903 (2010).
52. Li, W. et al. A natural allele of a transcription factor in rice confers broad-spectrum blast resistance. *Cell* **170**, 114–126.e115 (2017).

Acknowledgements

We thank Mawsheng Chern for critical reading and editing of the manuscript. This work was supported by grants from the National Key Research and Development Program (2021YFA1300702); National Natural Science Foundation of China (31922066, 32072043, 32272116) to J.W., (31825022, 32121003) to X.C., (32072407) to X.Z., (32072041) to J.Y.; China Agriculture Research System (CARS-01-1) to J.L.; and the Sichuan Science and Technology Program (2024NSFTD0022) to J.W., (2022ZDZX0012) to S.L., (2022JDTD0023) to J.F.

Author contributions

J.W., J.L. and X.C. conceived and designed the experiments. J.W., H.S., J.Y. and Z.Z. performed most of the experiments and prepared the figures. H.Yi, L.X., X.Z., H.T. and Q.X. contributed to pathogen inoculation assays. Xi.C., X.L., W.L., Y.T., Q.H., L.S., Y.L. and L.W. collected the data. H.Yu, J.F., C.S., T.L., P.Q., W.W., S.L., J.L., X.C. and J.W. analyzed the data. J.W., J.L., X.C., H.Yu and M.H. wrote the manuscript.

Competing interests

The authors declare no competing interests.

Additional information

Supplementary information The online version contains supplementary material available at https://doi.org/10.1038/s41467-024-51962-x.

Correspondence and requests for materials should be addressed to Jing Wang.

Peer review information *Nature Communications* thanks the anonymous, reviewer(s) for their contribution to the peer review of this work. A peer review file is available.